April 23, 2026

KURAMOTO MODEL OF SELF-SYNCHRONIZING OSCILLATORS

CLEVE MOLER (MOLER@MATHWORKS.COM) , INDIKA RAJAPAKSE (INDIKAR@UMICH.EDU) , AND STEVE SMALE (SMALE@MATH.BERKELEY.EDU)

Abstract. Yoshiki Kuramoto introduced his model of synchronized oscillators over 50 years ago. Since then, dozens of applications have been found. Most studies of the model itself incorporate probabilistic aspects and focus on behavior as the number of oscillators approaches infinity. In contrast, there is no randomness in our model or simulations, and we focus on a finite number of oscillators, $n = 4$ or 5. Our investigation of *potential flow* raises some unanswered questions.

Key words. Kuramoto, self-synchronizing, potential, oscillations

AMS subject classifications. 34-01 34-04, 34C15, 37C75, 37N30, 65L07, 65-04

1. Introduction.

Fireflies on a summer evening, pacemaker cells in the heart, neurons in the brain, a flock of starlings in flight, pendulum clocks mounted on a common wall, bizarre chemical reactions, alternating currents in a power grid, oscillations in SQUIDs (superconducting quantum interference devices). These are all examples of synchronized oscillators [9, 18, 24, 10, 4, 22, 7, 2, 14, 15, 23].

The scientific interest in synchronization of coupled oscillators can be traced back to the work by Huygens (1673) on "an odd kind of sympathy" between coupled pendulum clocks.

Inspired by Art Winfree [22], Yoshiki Kuramoto, Professor Emeritus of physics at Kyoto University, introduced the Kuramoto model. The Kuramoto model is a nonlinear dynamical system of coupled oscillators with specified natural frequencies. If the coupling is strong enough, the system will evolve to one with all oscillators in phase lock [5, 20]. Kuramoto published the first paper about this model in 1974 [11], and he was quite surprised when his model turned out to abstractly describe the dynamics of so many different physical systems [12, 3, 1]. In 2015, Kuramoto reminisced about the model in this YouTube video [13].

The heart, like all tissues, is composed of individual cells, primarily cardiac fibroblasts and cardiac muscle cells (myocytes) [16]. Interactions between and within these cells enable the heartbeat and pumping of blood throughout the body. If we grow these cells in a dish, we see myocytes beating independently. When mixed with cardiac fibroblasts, the beating becomes more pronounced. In addition, if the beating cells do not touch one another, their beats are independent - some are faster, some are slower. But after two or three days, the myocytes connect to form sheets of cells that beat in unison.

In another biological setting, synchronous firing patterns in certain regions of the brain are thought to be a root cause of movement disorders such as Parkinson's disease and essential tremor. One proven therapy for these disorders is deep brain stimulation (DBS), which delivers electrical impulses that disrupt the neural circuitry underlying these movements [21]. Individual manual adjustments to DBS parameters are made to find the most effective treatment. This setting is compatible with the Kuramoto model, which treats neurons as oscillators that synchronize, and may help explain features that lead to the development of abnormal neuronal firing patterns and pathology [8].

This manuscript is for review purposes only.

2. Kuramoto Model. The Kuramoto model is a system of n ordinary differential equations describing the time evolution, $\theta_k(t)$, of self-synchronizing oscillating components.

$$\frac{d\theta_k}{dt} = \omega_k + \frac{\kappa}{n}\sum_j \sin(\theta_j - \theta_k),\ k = 1, ..., n$$

Here, the ω_k are constants, the intrinsic frequencies of the oscillators, and the constant parameter κ is the coupling coefficient of the nonlinear synchronizing term.

Following Kuramoto's original paper, most investigations of this system incorporate some probabilistic aspects and are concerned with behavior as n goes to infinity. In contrast, there is no randomness in our model or simulation, and we focus on finite n, often $n = 4$ or 5.

All the figures presented in this paper were generated by a MATLAB program that simulates the Kuramoto model.

3. Potential. Define the potential by

$$v(\theta) = \sum_k \sum_{j>k} \sin^2 \frac{\theta_j(t) - \theta_k(t)}{2}$$

Then Kuramoto's equation can be written

$$\frac{d\theta}{dt} = \omega - \frac{\kappa}{n}\nabla v(\theta)$$

where $\nabla v = \frac{\partial v}{\partial \theta}$ is the gradient of the potential.

$$\frac{\partial v}{\partial \theta_k} = -\sum_j \sin(\theta_j - \theta_k)$$

If all the θ_k are equal, the oscillators are perfectly synchronized and $v(\theta) = 0$.

On the other hand, if $e^{i\theta_k}$ is distributed evenly around the unit circle, the oscillators are completely unsynchronized and $v(\theta)$ reaches a maximum, denoted by *vmax*.

4. Initial Condition. The initial state, shown in figure 1, has

$$\theta_k(0) = \frac{k}{n}2\pi,\ k = -\frac{n-1}{2}, ..., \frac{n-1}{2}$$

These $\theta_k(0)$ are in the *open* interval $(-\pi, \pi)$, separated from the endpoints by an amount that makes it possible to extend $e^{i\theta_k}$ to be periodic with period 2π. Consequently, $v(\theta)$ is at its maximum and the initial state is an unstable critical point.

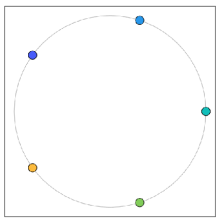

Fig. 1: Initial state, $\theta(0)$.

In a later section, we will discuss a modification of these initial conditions that we call *nudging*. It perturbs the values slightly to knock the system off the critical point.

5. Intrinsic Frequencies. The intrinsic frequencies, shown in figure 2, are constants controlled by a parameter σ that determines their *spread*.

$$\omega_k \;=\; \frac{k}{n-1} 2\sigma, k = -\frac{n-1}{2}, ..., \frac{n-1}{2}$$

These ω_k are distributed evenly in the *closed* interval $[-\sigma, \sigma]$. Half of the ω_k are positive, half are negative, and, if n is odd, one of them is zero.

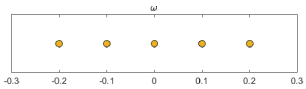

Fig. 2: Intrinsic Frequencies, ω.

If σ is zero, then all the ω_k are zero, and the dynamics are controlled by the synchronizing term. By taking $\kappa = n$ we have

$$\frac{d\theta}{dt} = -\nabla v(\theta)$$

This situation, which is known as *potential flow*, has interesting dynamics that we will examine in detail.

If both κ and σ are zero, the differential equations reduce to

$$\frac{d\theta}{dt} = 0$$

The solution is the constant initial condition

$$\theta(t) = \theta(0), \text{ for all } t.$$

Here are two typical solutions, each viewed from two different perspectives. The first point of view is a plot of $\theta(t)$ as a function of t. The initial values are always in the interval $(-\pi, \pi)$. The second point of view is snapshots from a video showing $e^{i\theta}$ move around the unit circle.

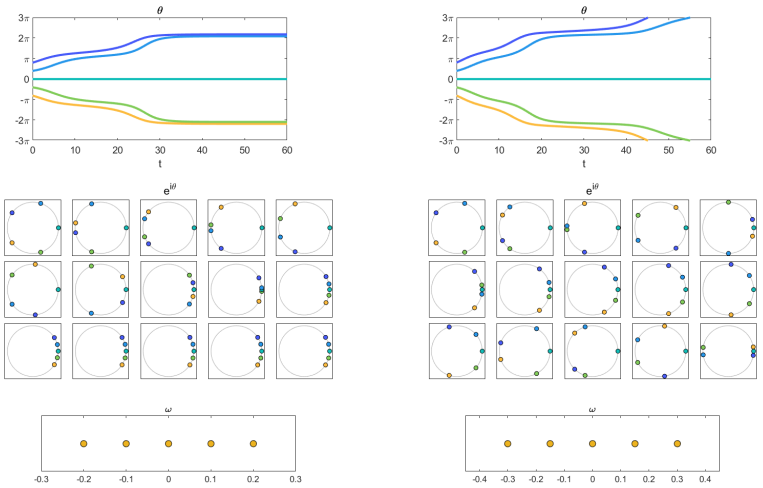

Fig. 3: Two behaviors of the Kuramoto system. (Left) Phase locked. (Right) Unstable.

6. Order Parameter. The *phase* θ_k is often identified with the point on the unit circle, the *frequency* $e^{i\theta_k}$ (Kuramoto synchronization index). In general the *order parameter* r and *average frequency*, ψ, are defined by

$$re^{i\psi} = \frac{1}{n}\sum_k e^{i\theta_k}$$

If the average is zero, then $r = 0$, but ψ is not uniquely defined.

The potential and the order parameter provide complementary measures of synchronicity; when one of them is equal to zero, the other is equal to one. In fact, we now know a quantitative relationship between the two.

$$\begin{aligned} v &= \frac{4}{n^2}\sum_k\sum_{j>k}\sin^2((\theta_j-\theta_k)/2) \\ &= \frac{4}{n^2}\sum_k\sum_{j>k}\left(\frac{1-\cos(\theta_j-\theta_k)}{2}\right) \\ &= \frac{n-1}{n}-s \end{aligned}$$

$$\text{where } s=\frac{2}{n^2}\sum_k\sum_{j>k}\cos(\theta_j-\theta_k)$$

$$\begin{aligned} r^2 &= \left|\frac{1}{n}\sum_{k=1}^{n}e^{i\theta_k}\right|^2 \\ &= \frac{1}{n^2}\left(\sum_k\cos(\theta_k)\right)^2+\frac{1}{n^2}\left(\sum_k\sin(\theta_k)\right)^2 \\ &= \frac{1}{n}+s \end{aligned}$$

Consequently

$$v+r^2=1$$

7. Overview. Three parameters control this model: n, the number of oscillators, κ, the strength of the synchronizing term, and σ, the spread of the natural frequencies, ω.

For each n, the κ - σ plane shown in figure 4 is divided into two regions, stable and unstable. The dividing line is known as *critical coupling*.

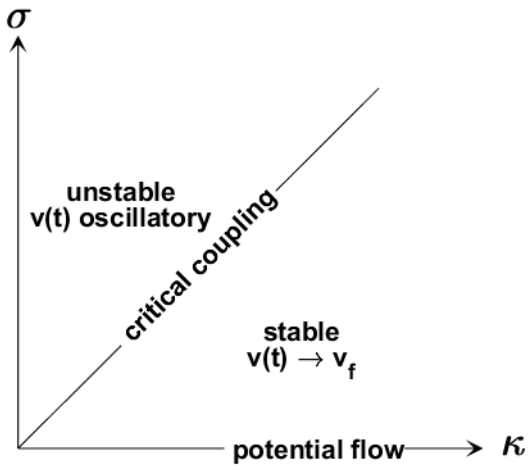

Fig. 4: Overview

When σ is above the critical line in the κ - σ plane, the linear term involving ω dominates. The system is always unstable in the sense that the oscillators fail to synchronize, and the potential $v(t)$ does not approach a limit.

When σ is below the critical line, but not on the κ-axis, the nonlinear synchronizing term dominates. The system is stable, and the potential always reaches a non-zero limiting value, $v(t) \to vmax$. This limiting value is near one if σ is near the critical line and near zero if σ is near the κ-axis. The oscillators do not completely synchronize, but reach *phase lock*.

We call the situation when $\sigma = 0$ "potential flow". All of the natural frequencies ω_k are zero. With $\kappa = 2/n$, the Kuramoto equation becomes

$$\frac{d\theta}{dt} = -\nabla v(\theta)$$

The gradient of the potential completely determines the dynamics. The initial condition θ_0 equally distributed in $(-\pi, \pi)$ is an unstable critical point. We consider potential flow in detail in a later section.

8. Critical Coupling. The two parameters κ and σ represent competing forces. Increasing σ increases the spread of the natural frequencies, ω, thereby promoting less synchronization. Countering that, increasing κ increases the strength of the nonlinear synchronizing term. Having the two balance each other is *critical coupling*.

We use two scalar functions derived from the state $\theta(t)$ to assess the synchronization. One is the potential, $v(t)$; the other is the norm of the derivative,

$$\mu(t) = ||\frac{d\theta}{dt}||$$

A system is *stable* if it reaches a time t where $\mu(t) < \text{tol}$, with $\text{tol} = 10^{-4}$. It is

unstable if the time t reaches a limit t_f without achieving stability.

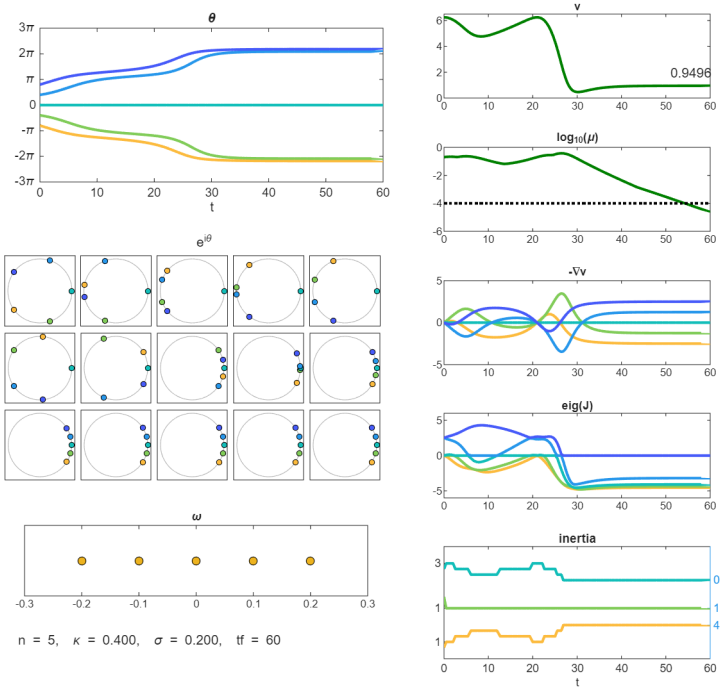

Fig. 5: The configuration with $\sigma = 0.200$ is stable and reaches phase-locked equilibrium.

Figure 5 shows the behavior of several variables in a typical stable situation. The values of the parameters are:

```
n = 5;
kappa = 0.400;
sigma = 0.200;
tf = 60;
```

The plots of the five functions $\theta_k(t)$, $k = 1, ..., 5$, reach constant limiting values as $t \to \infty$, but not, as might be expected, to values near each other. The two blue plots have positive initial values between 0 and π; They speed up and reach limits greater than 2π. The green and gold plots start with negative initial values. They slow down and approach limiting values below -2π. The middle plot starts at 0 and stays there.

The snapshots show the motion of the $e^{i\theta_k(t)}$ around the unit circle. The blue dots move counter-clockwise while the green and gold dots move clockwise. All five dots eventually settle down at positions near, but not exactly on, $(1, 0)$. The subplot on the lower left of figure 5 shows the five constant intrinsic frequencies ω_k equally spaced in $[-\sigma, \sigma]$.

The first subplot on the right shows the potential v. After some initial fluctuations, v settles down, and the limiting value, v_f, is shown on the far right. The second

subplot shows μ, the norm of the derivative of v. The value of $\log_{10}(\mu)$ drops below the line at -4 near $t = 50$, indicating stability, and the first two subplots are green as a result.

The next subplot shows the gradient of the potential, $-\nabla v$.

The last two subplots show the eigenvalues of the Jacobian matrix, and the *inertia*, the number of positive, zero and negative eigenvalues.

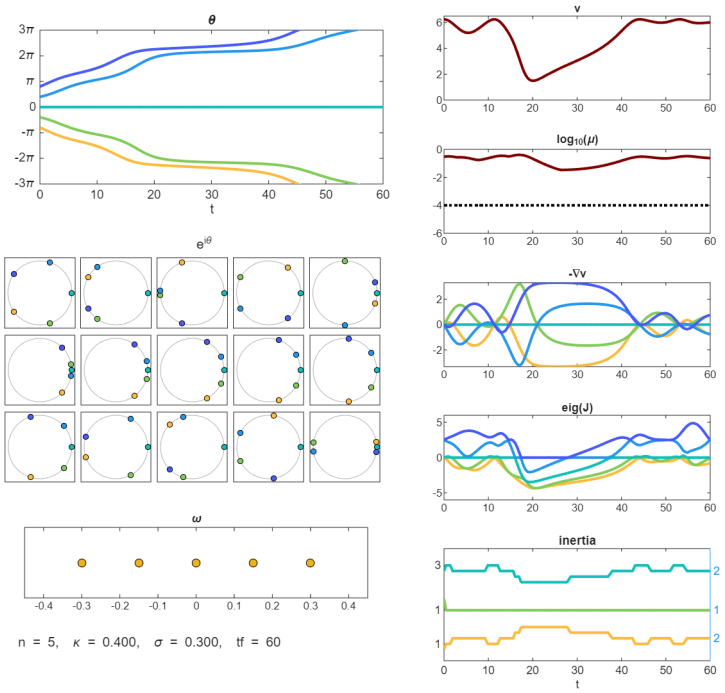

Fig. 6: The configuration with $\sigma = 0.300$ is unstable.

Figure 6 has σ increased to 0.300. This is beyond the critical coupling point. thereby producing instability. The θ's diverge, and the potential v oscillates. The plot is red; v_f is undefined.

9. Jacobian and Inertia. The Jacobian of v is the matrix

$$J_{k,j} = \frac{\partial^2 v}{\partial \theta_k \partial \theta_j}$$

The *inertia* of a symmetric matrix is a triple [6]

$$[t_+, t_0, t_-]$$

where

$$
\begin{aligned}
t_+ &= \text{number of positive eigenvalues} \\
t_0 &= \text{number of zero eigenvalues} \\
t_- &= \text{number of negative eigenvalues}
\end{aligned}
$$

The inertia of the Jacobian varies during the motion. The final value characterizes the stability.

In figure 5, none of the final eigenvalues are positive, the inertia is [0,1,4]and the motion is stable. In figure 6, two of the eigenvalues are positive, the inertia is [2,1,2] and the motion is unstable. We will see more examples in the section on potential flow.

There is a close connection between matrix inertia and Morse index theory. Let $\mathbf{H}(x^*)$ be the Hessian of a potential function at a critical point x^*. The Morse index, defined as the number of positive eigenvalues of $\mathbf{H}(x^*)$, determines the dimension of the unstable manifold and provides a qualitative topological picture of the dynamics near x^*.

10. Strogatz. Steven Strogatz, in an overview of work on Kuramoto oscillators, provided two sketches illustrating the behavior of the order parameter, $r(t)$ [17, 19]. His first sketch shows the evolution of $r(t)$ as a function of t for values of the coupling parameter above and below the critical value. As Kuramoto did in his original paper 25 years earlier, Strogatz is thinking of n approaching infinity. If $K < K_c$, there is not enough coupling to force stabilization, and $r(t)$ approaches zero. But $K > K_c$, the coupling overcomes the disparity in the natural frequencies and $r(t)$ approaches an upper limit [7].

If he followed our color conventions, the upper curve ($K > K_c$) in this sketch would be green and the lower curve ($K < K_c$) would be red.

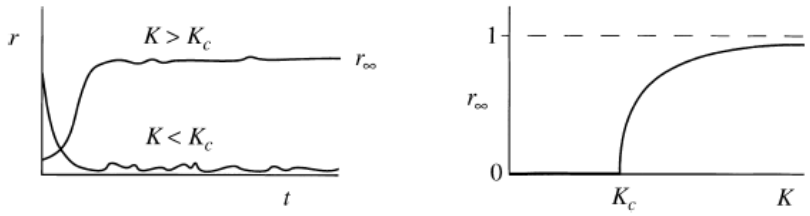

Fig. 7: (A) Strogatz's first sketch. (B) Strogatz's second sketch. These are copies of Figs. 2 and 3 from Strogatz 2001.

In his second sketch (figure 7B), Strogatz shows the behavior of the order parameter above and below critical coupling.

11. Bisection. We can use bisection to compute the critical coupling point for a given n and either κ or σ.

Assume n and κ are fixed. We know from experience that the critical σ is between $\kappa/2$ and κ. Here is an outline of an algorithm to find σ.

```
a = kappa/2
b = kappa
```

```
while b-a > tol
    sigma = (a + b)/2
    compute the solution for this kappa and sigma
    if solution is stable
        a = sigma
    else
        b = sigma
    end
end
```

For example, $n = 5$ and $\kappa = 0.300$. Starting with a = .150 and b = .300, bisection generates

```
0.2250
0.1875
0.2062
0.1969
0.1922
0.1898
0.1910
0.1916
0.1919
0.1917
0.1917
0.1916
```

A similar algorithm takes a fixed n and σ and finds the critical value for κ.

12. Approaching stability. Here are our versions of the Strogatz sketches.

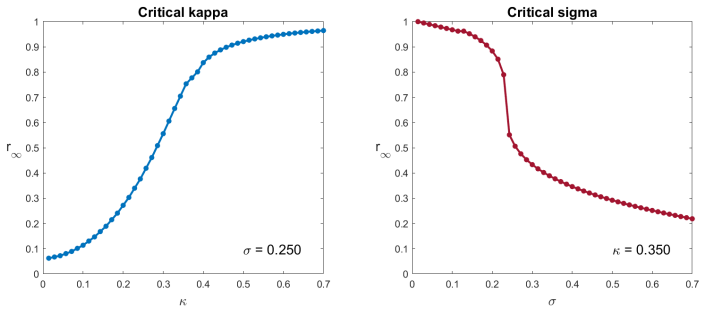

Fig. 8: Approaching stability

13. Potential flow. In potential flow, all the ω_k are zero. The initial conditions for $\theta(0)$ allow $e^{i\theta(0)}$ to be equally spaced around the unit circle. We perturb these initial conditions by $\rho\nu$, where ρ is a scalar controlling the magnitude of the perturbation and ν is a vector of positive ones, negative ones and zeros.

Table 1 shows the results. We would like to characterize the number of sources, saddles, and sinks for each n using properties of the subgroups of the rotation group of n points.

For a few perturbations, $\theta_k(t)$ remains a source. The potential is at its maximum. Figure 9 is an example.

If n is prime, there are only three such perturbations: all positive, all zero, and

n	3^n	sink	saddle	source
2	9	6	0	3
3	27	21	3	3
4	81	68	4	9
5	243	220	20	3
6	729	678	18	33
7	2187	2093	91	3
8	6561	6384	96	81
9	19683	19305	351	27
10	59049	58440	360	249
11	177147	175813	1331	3
12	531441	528984	1368	1089
13	1594323	1589640	4680	3
14	4782969	4775862	4914	2193
15	14348907	14332440	16200	267

Table 1: Sources, saddles, and sinks.

all negative.

If n is prime, the rotation group is simple.

For n a power of 2, the number of sources is $3^{n/2}$, that is, 3, 9, 81, 6561, etc.

For a few other perturbations, θ approaches a saddle. Figure 10 is an example.

The potential approaches a nonzero limit. For all the saddles we know about, all the $e^{i\theta_k}$ except one converge to the same point on the unit circle. The lone exception converges to the opposite point on the circle. (In many cases, it didn't have to move.) Without loss of generality, we can say the exception has index $k = n$ and the limit is $\theta_n(t)$ is π. All the others, with indices 1 through $n-1$, converge to zero. The limiting potential is $n - 1$.

Most perturbations produce a sink. Figure 11 is an example.

14. Conclusion. We do not yet have a complete understanding of table 1 and its extension to larger numbers of oscillators. Further investigation is required.

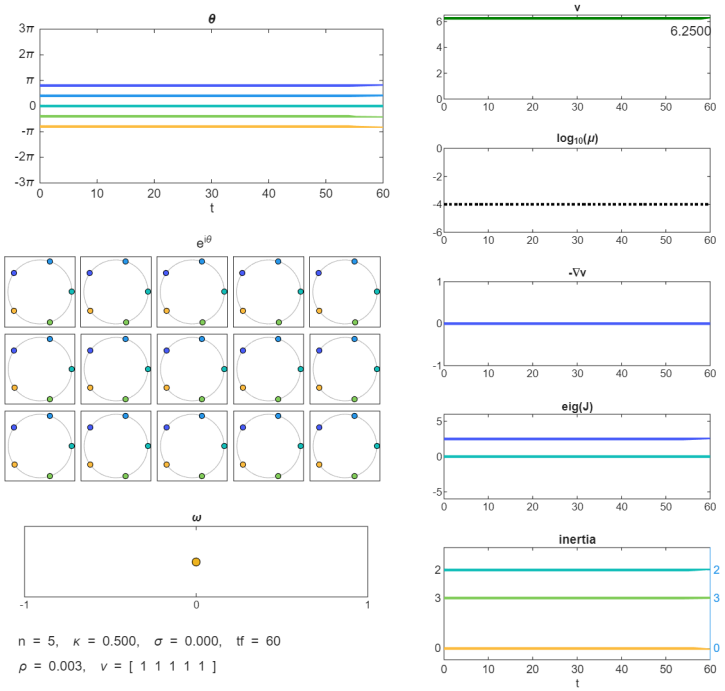
θ
t
e^{iθ}
ω
v
6.2500
log10(μ)
-∇v
eig(J)
inertia
t
n = 5, κ = 0.500, σ = 0.000, tf = 60
ρ = 0.003, v = [1 1 1 1 1]

Fig. 9: Source.

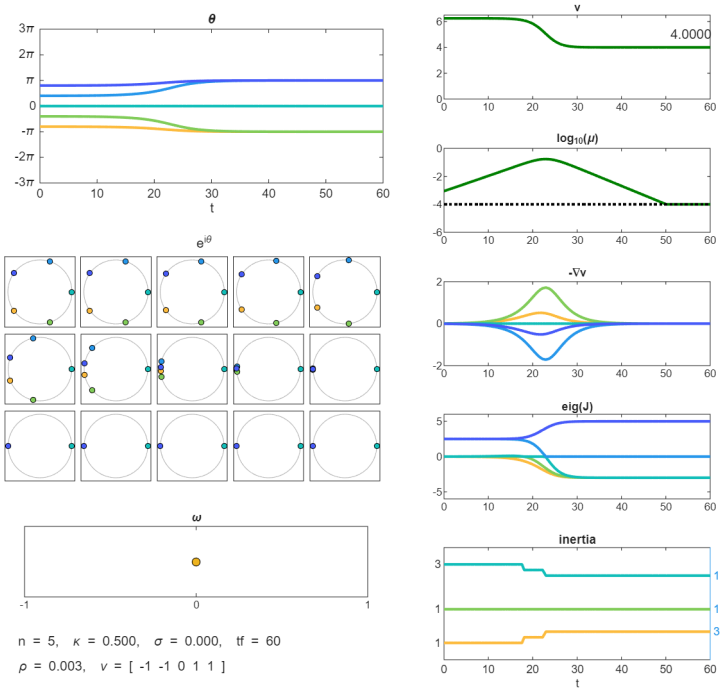

Fig. 10: Saddle.

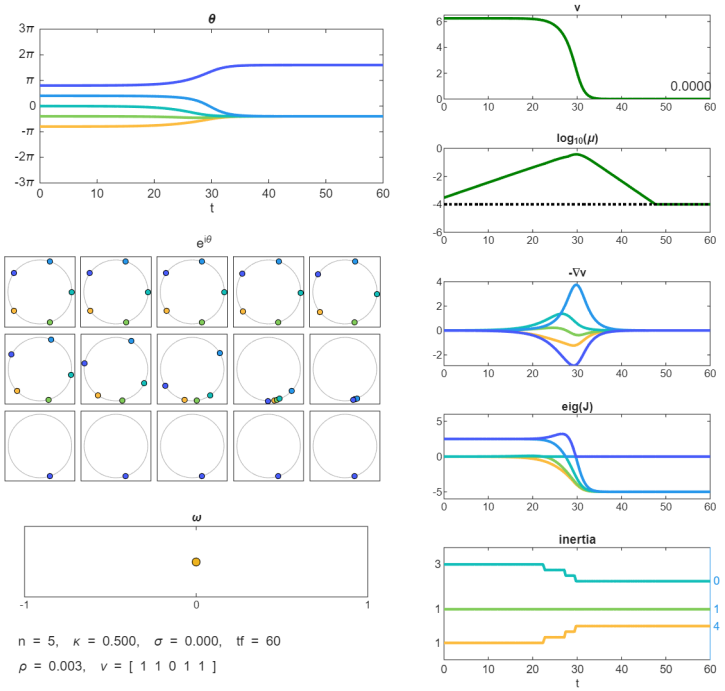
θ
3π
2π
π
0
-π
-2π
-3π
0 10 20 30 40 50 60
t
v
6
4
2
0
0.0000
0 10 20 30 40 50 60
log10(μ)
0
-2
-4
-6
0 10 20 30 40 50 60
eiθ
-∇v
4
2
0
-2
0 10 20 30 40 50 60
eig(J)
5
0
-5
0 10 20 30 40 50 60
ω
-1
0
1
inertia
3
1
1
0
1
4
0 10 20 30 40 50 60
t
n = 5, κ = 0.500, σ = 0.000, tf = 60
ρ = 0.003, v = [1 1 0 1 1]

Fig. 11: Sink.

241 REFERENCES

242 [1] J. A. Acebrón, L. L. Bonilla, C. J. P. Vicente, F. Ritort, and R. Spigler, *The kuramoto*
243 *model: A simple paradigm for synchronization phenomena*, Reviews of modern physics, 77
244 (2005), p. 137.
245 [2] M. Bennett, M. F. Schatz, H. Rockwood, and K. Wiesenfeld, *Huygens's clocks*, Proceed-
246 ings of the Royal Society of London. Series A: Mathematical, Physical and Engineering
247 Sciences, 458 (2002), pp. 563–579.
248 [3] F. Dörfler and F. Bullo, *Synchronization in complex networks of phase oscillators: A*
249 *survey*, Automatica, 50 (2014), pp. 1539–1564.
250 [4] F. Dörfler, M. Chertkov, and F. Bullo, *Synchronization in complex oscillator networks*
251 *and smart grids*, Proceedings of the National Academy of Sciences, 110 (2013), pp. 2005–
252 2010.
253 [5] G. B. Ermentrout, *Synchronization in a pool of mutually coupled oscillators with random*
254 *frequencies*, Journal of Mathematical Biology, 22 (1985), pp. 1–9.
255 [6] G. H. Golub and C. F. Van Loan, *Matrix Computation, Fourth Edition*, The John Hopkins
256 University Press, 2013.
257 [7] O. A. Heggli, J. Cabral, I. Konvalinka, P. Vuust, and M. L. Kringelbach, *A kuramoto*
258 *model of self-other integration across interpersonal synchronization strategies*, bioRxiv,
259 (2019), p. 640383.
260 [8] F. C. Hoppensteadt and E. M. Izhikevich, *Weakly connected neural networks*, vol. 126,
261 Springer Science & Business Media, 2012.
262 [9] C. Huygens, *Oeuvres complètes de Christiaan Huygens*, vol. 8, M. Nijhoff, 1899.
263 [10] I. Z. Kiss, Y. Zhai, and J. L. Hudson, *Emerging coherence in a population of chemical*
264 *oscillators*, Science, 296 (2002), pp. 1676–1678.
265 [11] Y. Kuramoto, *International symposium on mathematical problems in theoretical physics*, Lec-
266 ture notes in Physics, 30 (1975), p. 420.
267 [12] ———, *Chemical oscillations, waves, and turbulence*, Courier Corporation, 2003.
268 [13] ———, *Kuramoto talks about the kuramoto model*, Youtube, (2015).
269 [14] A. Pikovsky, M. Rosenblum, and J. Kurths, *Synchronization: a universal concept in non-*
270 *linear science*, 2002.
271 [15] H. Schmidt, G. Petkov, M. P. Richardson, and J. R. Terry, *Dynamics on networks: the*
272 *role of local dynamics and global networks on the emergence of hypersynchronous neural*
273 *activity*, PLoS computational biology, 10 (2014), p. e1003947.
274 [16] D. Srivastava and N. DeWitt, *In vivo cellular reprogramming: the next generation*, Cell,
275 166 (2016), pp. 1386–1396.
276 [17] S. Strogatz, *From kuramoto to crawford: exploring the onset of synchronization in popula-*
277 *tions of coupled oscillators*, Physica D: Nonlinear Phenomena, 143 (2000), pp. 1–20.
278 [18] ———, *Sync: The emerging science of spontaneous order*, Penguin UK, 2004.
279 [19] S. Strogatz and I. Stewart, *Coupled oscillators and biological synchronization*, Scientific
280 American, 269 (1993), pp. 102–109.
281 [20] J. Van Hemmen and W. Wreszinski, *Lyapunov function for the kuramoto model of nonlinearly*
282 *coupled oscillators*, Journal of Statistical Physics, 72 (1993), pp. 145–166.
283 [21] G. Weerasinghe, B. Duchet, H. Cagnan, P. Brown, C. Bick, and R. Bogacz, *Predict-*
284 *ing the effects of deep brain stimulation using a reduced coupled oscillator model*, PLoS
285 computational biology, 15 (2019), p. e1006575.
286 [22] A. T. Winfree, *Biological rhythms and the behavior of populations of coupled oscillators*,
287 Journal of theoretical biology, 16 (1967), pp. 15–42.
288 [23] ———, *The geometry of biological time*, vol. 12, Springer Science & Business Media, 2001.
289 [24] ———, *On emerging coherence*, Science, 298 (2002), pp. 2336–2337.